Monatshefte für Chemie 133, 785–798 (2002)

**Monatshefte für Chemie**
**Chemical Monthly**


# Growth of Anodic Films on Compound Semiconductor Electrodes: InP in Aqueous $(NH_4)_2S$

**Denis N. Buckley**[1,*], **Elizabeth Harvey**[1], and **Sung-Nee G. Chu**[2]

[1] Department of Physics and Materials and Surface Science Institute, University of Limerick, Ireland
[2] Agere Systems, Murray Hill, NJ, USA

**Summary.** Film formation on compound semiconductors under anodic conditions is discussed. The surface properties of InP electrodes were examined following anodization in an $(NH_4)_2S$ electrolyte. The observation of a current peak in the cyclic voltammetric curve was attributed to selective etching of the substrate and a film formation process. AFM images of samples anodized in the sulfide solution revealed surface pitting. Thicker films formed at higher potentials exhibited extensive cracking as observed by optical and electron microscopy, and this was explicitly demonstrated to occur *ex situ* rather than during the electrochemical treatment. The composition of the thick film was identified as $In_2S_3$ by EDX and XPS. The measured film thickness varies linearly with the charge passed, and comparison between experimental thickness measurements and theoretical estimates for the thickness indicate a porosity of over 70%. Cracking is attributed to shrinkage during drying of the highly porous film and does not necessarily imply stress in the wet film as grown. During the growth of the thick porous film, spontaneous current oscillations have been observed. The frequency of oscillation was found to be proportional to the current density, regardless of whether the measurements were carried out during a potential sweep or at constant potential. Thus, the charge passed per oscillation remained constant. A characteristic value of approximately $0.3\,C \cdot cm^{-2}$ was measured under potential sweep conditions, and a similar value was obtained at constant potential.

**Keywords.** InP; Anodic films; Oscillations; Cyclic voltammetry; Electron microscopy.

## Introduction

Group III–V semiconductors are widely used for optoelectronic devices and for high power and high speed electronic devices. However, passivation of the semiconductor is required to overcome some of the device problems which are associated with surface states, such as catastrophic optical damage in lasers [1] and low current gain in heterojunction bipolar transistors (HBTs) [2]. Study of the anodic growth of films on III–V semiconductors such as InP [3] and GaAs [4] has stemmed from their potential use as insulating layers in metal-insulator

* Corresponding author. E-mail: noel.buckley@ul.ie

semiconductor (MIS) devices with better electrical results being achieved when a passivation step is carried out prior to growth of the anodic film [5, 6]. Photoenhanced oxidation of GaN has been found to result in an increase in photoluminescence intensity, thus indicating the passivating nature of the surface oxide formed in this case [7]. Metal-oxide semiconductor (MOS) structures using photo-electrochemically formed oxide layers on GaN have been fabricated [8], and interesting features such as cracking of the oxide film formed have also been reported for the case of GaN [7].

There is considerable interest in the role of sulfur as a passivating species [9–11]. Sulfur treatment has been shown to considerably improve surface properties of III–V semiconductors [12–14]. In particular, anodic films grown in sulfur-containing electrolytes appear to result in surfaces which are more resistant to reoxidation [15, 16]. However, cracking of the anodically grown surface film on a p-InP electrode in a sulfur-containing electrolyte has been reported [17].

The observation of current oscillations during the anodization of CdTe [18], HgTe [19], and CdHgTe [20] in sulfide solutions has been reported. Anodic oscillations have also been observed in n-GaAs under conditions of strong illumination in a borax solution [21] and in both p-type [22] and n-type [23] Si, mainly in fluorine-containing electrolytes. More recently, potential oscillations have been noticed during galvanostatic anodization of n-InP in HCl [24]. Cases of oscillatory behaviour have been reported for other semiconductor/electrolyte systems [25] and for many metal/electrolyte systems [26–28].

Thus, the nature of anodic processes on compound semiconductors, the formation of films, their structure and composition, and the relationship to growth conditions are important, both from a fundamental and a technological point of view. It seems worthwhile to gain deeper insight into the factors governing the electrochemical reactions, the film growth kinetics and behaviour, the morphology, and other properties of the films formed in order to understand the mechanism of dissolution, film growth, and oscillatory behaviour of compound semiconductors.

Due to the above mentioned interest in interfaces between compound semiconductors and sulfur-containing electrolytes we have chosen to use InP electrodes in aqueous sulfide solutions as a model system to investigate their behaviour [29, 30]. In this paper we report on the results of an investigation of the growth of anodic films in this system. We elucidate the nature of previously reported cracking of these films and communicate observations of electrochemical oscillations.

## Results and Discussion

### *Film growth at lower potentials*

Figure 1 shows cyclic voltammograms of an InP electrode in a $3\,\mathrm{mol}\cdot\mathrm{dm}^{-3}$ $(NH_4)_2S$ electrolyte. The potential was scanned at a rate of $10\,\mathrm{mV}\cdot\mathrm{s}^{-1}$ between an initial value of 0.0 V and upper potentials ($E_U$) of 0.785 and 0.88 V, respectively. When $E_U$ was less then the peak potential $E_P$, the value of the current on the return scan was roughly similar to the corresponding current on the forward scan (Fig. 1a). The current-voltage characteristics obtained for $E_U = 0.88\,\mathrm{V}$ (*i.e.* above the peak potential) are shown in Fig. 1b. In this case, the current density on the cathodic

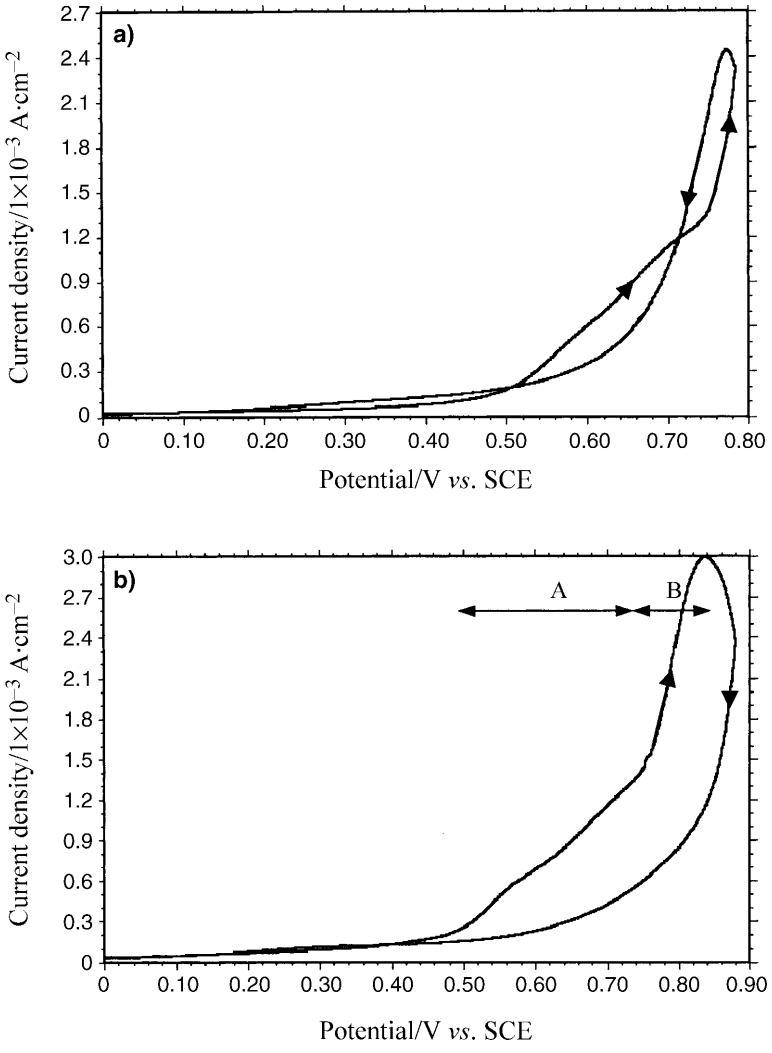


**Fig. 1.** Cyclic voltammograms of InP in $3\,\text{mol}\cdot\text{dm}^{-3}$ $(NH_4)_2S$ at a scan rate of $10\,\text{mV}\cdot\text{s}^{-1}$ between 0.0 V (SCE) and a) $E_U = 0.785$ V (SCE) b) $E_U = 0.88$ V (SCE)

scan was considerably lower than on the anodic scan. Such results suggest that the peak in current density corresponds to passivation of the surface by a deposited film which also inhibits current flow on the cathodic scan.

Atomic force microscopy (AFM) was used to investigate the topography of the InP electrodes following different anodization procedures. Figure 2 shows a 500 nm × 500 nm AFM image of a sample that was subjected to a linear sweep from 0.0 V to a value of $E_U = 0.785$ V. On careful inspection it can be seen that small holes or pits are dispersed over the surface of the sample. Larger areas of the same electrode were imaged, and these pits were found to exist over the whole surface. This indicates that selective etching of the InP substrate occurs in region B of Fig. 1b. If the potential was scanned back to 0.0 V, an increase in the pit density was observed. Thus, selective etching of the InP electrode also occurs on the return scan.

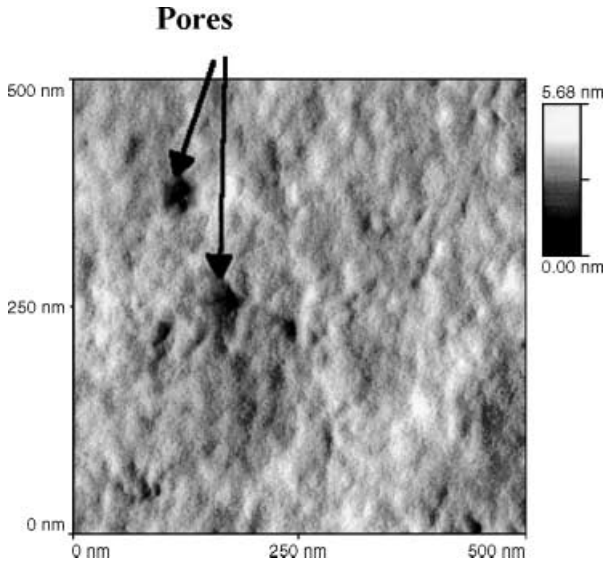


**Fig. 2.** AFM image of an n-InP sample scanned from 0.0 to 0.785 V (SCE) at $10\,\mathrm{mV}\cdot\mathrm{s}^{-1}$ in $3\,\mathrm{mol}\cdot\mathrm{dm}^{-3}$ $(NH_4)_2S$

The surface topography was also examined after a sample had undergone anodization up to 0.7 V. However, no pits were observed in the AFM images taken. In order to investigate whether more prolonged treatment would accentuate pit formation, samples were subjected to repeated cycling between 0.0 V and 0.7 V. Even after such treatment, no obvious pits were observed in the AFM images, although the surface was found to have a much rougher texture than that of an untreated electrode. Thus, the onset of pit formation in the InP surface appears to correspond to the rapid rise in current in the potential region indicated as B in Fig. 1b.

The topography of samples subjected to a potential cycle between 0.0 V and $E_U$ values of 0.82 V (*i.e.* peak potential) and 0.88 V, respectively, was examined, and it is clear from a comparison of the AFM images obtained that the density of pits continues to increase over the potential range from 0.75 to 0.88 V. Thus, it appears that at potentials between 0.5 and 0.75 V etching of the InP occurs with the development of a characteristic surface texture but with no pit formation. Above 0.75 V, pits are formed in the InP surface with a consequent accelerated increase in current. Comparison of AFM images corresponding to potential cycling to 0.82 and 0.88 V shows a change in texture, probably due to the growth of a thicker surface film (35 nm at 0.88 V). The decrease in current following the peak at $E_P$ and the subsequent reduced current on the reverse scan is indicative of the growth of a film. However, the amount of decrease in current is relatively small, consistent with the porosity in the film. The results indicate that films grown under such conditions, while exhibiting some degree of passivity, are not effective as passivating layers.

### *Film growth at higher potentials*

Figure 3 shows a cyclic voltammogram at a scan rate of $10\,\mathrm{mV}\cdot\mathrm{s}^{-1}$ from 0 to 2.2 and back to 0 V. It exhibits two noteworthy features. Firstly, it is apparent that

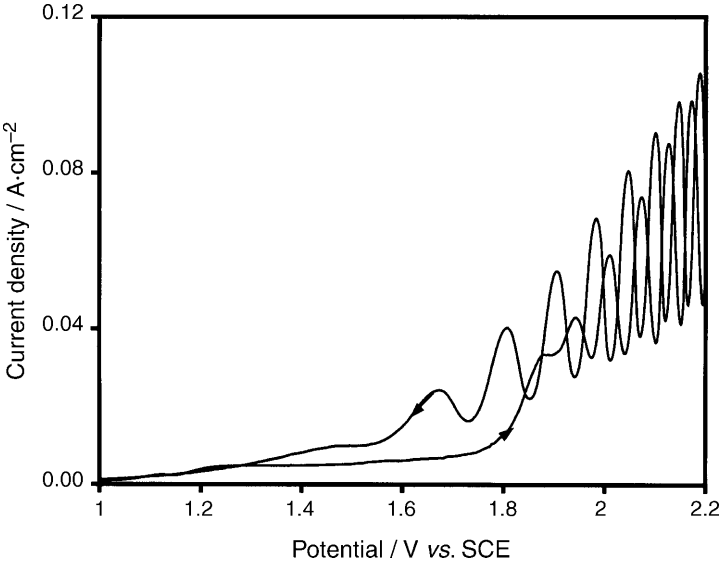


**Fig. 3.** Cyclic voltammogram of InP between 0.0 and 2.2 V (SCE) in 3 mol · dm$^{-3}$ $(NH_4)_2S$ at a scan rate of 10 mV · s$^{-1}$

current oscillations occur in the anodic scan at potentials above 1.7 V; this feature will be discussed later. Secondly, the current on the cathodic sweep is, in general, greater than the corresponding (average) current on the anodic scan.

This contrasts with observations at lower potentials (cf. Fig. 1b) and suggests that the films formed at higher potentials are not passivating in nature. Electrodes exposed to potential cycles such as in Fig. 3 and subsequently removed from the cell and examined by scanning electron and optical microscopy clearly showed a pattern of cracking of the surface film. Figure 4 presents a scanning electron micrograph (SEM) surface view of a typical film formed as a result of a cyclic potential sweep between 0.0 and 1.95 V. Extensive cracking of the film is obvious from this micrograph.

To investigate further the origin of this cracking, an InP electrode was subjected to a cyclic potential sweep between 0 and 2.4 V. The electrode was rinsed in deionized water and quickly transferred while still wet to a container in which the relative humidity was maintained at approximately 100%. The sample was then quickly transferred from the container to the optical microscope stage and immediately examined. A time sequence of images obtained as the sample was allowed to dry in ambient laboratory air is shown in Fig. 5. The first image obtained (Fig. 5a) shows that initially the surface was essentially featureless at this magnification, with no evidence of surface cracking. However, after a few minutes (Fig. 5b), cracks appeared in the film. The progression of film cracking was monitored over a period of approximately 20 minutes, and it is obvious from the images in Figs. 5a through 5d taken over this time period that crack formation and broadening continued as the sample was allowed to dry. We attribute the formation of the cracks observed to a shrinkage of the film as it dries. As shown below, the film involved is highly porous, and this is expected to enhance the shrinkage when water is lost by evaporation. Clearly, the surface cracking occurs *ex situ* and is

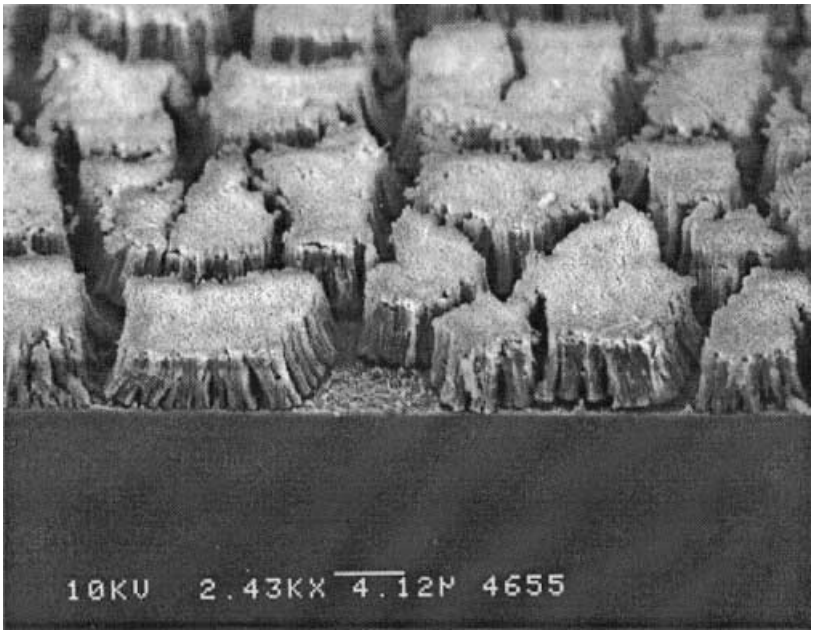


**Fig. 4.** SEM showing the characteristic cracking of the film formed after a cyclic potential sweep between 0.0 and 1.95 V (SCE) in $3\,\text{mol}\cdot\text{dm}^{-3}$ $(NH_4)_2S$ at a scan rate of $10\,\text{mV}\cdot\text{s}^{-1}$

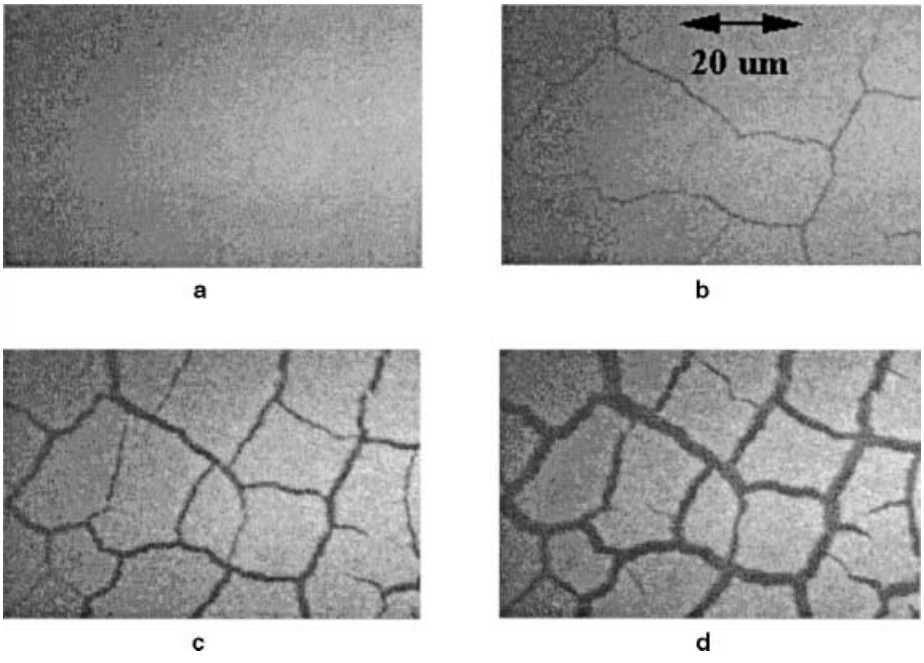


**Fig. 5.** Time-lapse sequence of optical micrographs showing the evolution of surface cracks on a film as it dries; (a) through (d) were taken sequentially over a 20 min period; the film was formed by cycling the electrode between 0.0 and 2.4 V (SCE) in $3\,\text{mol}\cdot\text{dm}^{-3}$ $(NH_4)_2S$ at a scan rate of $10\,\text{mV}\cdot\text{s}^{-1}$

not a property of the film during the electrochemical treatment. It appears that the cracking occurs due to stress induced by drying of the highly porous film and does not necessarily imply stress in the wet film as grown. We have also observed similar cracking of films formed on p-InP at high anodic potentials. Such cracks have been reported previously [17] in the case of anodization of a p-InP surface in aqueous $(NH_4)_2S$, but their formation was ascribed to stress that occurs in the surface film during anodization. In view of the present results, however, this would not appear to be the origin of this cracking.

Cross sections of the electrode were prepared by cleaving the InP substrate along the (110) crystal plane and allowing the film to break along the cleavage plane of the underlying substrate. The cracks apparent in the surface micrographs are also evident in these cross sections and are observed to extend, typically, through the full thickness of the film.

The elemental composition of films was investigated using both energy dispersive X-ray analysis (EDX) and X-ray photoelectron spectroscopy (XPS). In order to eliminate any effect due to signals from In and P in the underlying InP, samples of the film were detached from the substrate and examined. Spectra obtained from such detached films show that S and In are the predominant elements in the film, whereas P appears to be present only in small quantities. The In:P atomic ratio was calculated for two samples in which the film had been detached. When a correction was made for P assumed to be present as InP, an average value of 0.65 was obtained for the In:S ratio in the film. This is in reasonable agreement with the calculated value of 0.67 corresponding to $In_2S_3$. XPS measurements were carried out on a sample which had been subjected to a potential sweep from 0.0 to 1.8 V. The In 3d5/2 peak obtained from the surface film is shifted to a higher binding energy relative to the corresponding peak obtained from the substrate. This shift in binding energy was measured to be 0.4 eV and indicates a change in the bonding structure of In: it is consistent with In present as $In_2S_3$ [31]. In summary, the EDX and XPS measurements suggest that, in agreement with previous reports [17], the film consists predominantly of $In_2S_3$.

*Film porosity*

Film thicknesses were obtained from cross-sectional optical and electron micrographs of dry films. The samples were subjected to a cyclic potential scan from 0 V to a series of values of upper potentials greater than 1.7 V (and back to 0 V). The total charge density ($Q$) passed during the cyclic potential sweep was determined by estimating the integral of the current with respect to time from the total area (forward and backward sweeps) under the cyclic voltammogram curve. This charge was estimated for each of the samples used in the thickness measurement study. Estimates obtained in this way clearly show that the measured film thickness is proportional to the charge passed, and a value of $1.64\,\mu m \cdot C^{-1} \cdot cm^2$ is obtained for the ratio of measured film thickness to charge. The fact that the film thickness increases linearly with the charge passed indicates that a constant percentage porosity is maintained.

A theoretical value for the ratio of film thickness to charge passed during film growth was also estimated. We assume an electrochemical process such as given in

Eq. (1) leading to the formation of an $In_2S_3$ film and dissolved oxo anions of phosphorous.

$$InP + 3/2\,S^{2-} + 4H_2O + 8h^+ \longrightarrow 1/2In_2S_3 + PO_4^{3-} + 8H^+ \quad (1)$$

The formation of $PO_4^{3-}$ (a P(V) oxo anion) as written in Eq. (1) corresponds to an 8-electron process, whereas, for example, the formation of a P(III) oxo anion such as $HPO_3^{2-}$ corresponds to a 6-electron process. For a compact film, using *Faraday*'s law, the ratio of the thickness $d$ to the charge $Q$ is given by Eq. (2) where $V_{M(In_2S_3)}$ is the molar volume of $In_2S_3$, $n$ is the number of holes per formula unit of InP, and $F$ is the Faraday constant.

$$\frac{d}{Q} = \frac{V_{M(In_2S_3)}}{2nF} \quad (2)$$

Using a value of $73.17\,cm^3 \cdot mol^{-1}$ for $V_{M(In_2S_3)}$ [32] and assuming $n = 8$, a theoretical value of $0.474\,\mu m \cdot C^{-1} \cdot cm^2$ is estimated from Eq. (2) for $d/Q$, the ratio of (compact) film thickness to charge. As indicated above, an estimate of $1.64\,\mu m \cdot C^{-1}$ was obtained for the corresponding ratio $d_e/Q$ of experimental film thickness $d_e$ to charge, and thus the as-measured film thickness is found to exceed the estimated value for a compact film by a factor of $r = 3.46$, indicating that the film is highly porous. Using the estimated value of $r = 3.46$, we obtain an estimate of film porosity of approximately 71%. It is clear from Fig. 4 that lateral shrinkage (and hence cracking) of the film occurs. From surface-view micrographs, quantitative estimates of the degree of shrinkage were achieved [33]. Talking this into account we obtain a corrected value of porosity $p = 78\%$. As stated above, this assumes an 8-electron process: assuming a 6-electron process leads to a value of $r = 2.59$ and a porosity of 71%. Thus, we estimate the porosity to be in the range 71–78%.

It is clear that films formed at potentials above 1.7 V are quite porous. Film growth mechanisms on semiconductors including Si [34], GaAs [35], and InP [36] are often associated with the drift of ionic species through the anodic film under the influence of an electric field. While such a mechanism may operate for film growth at lower potentials in the present InP/S system, at higher potentials we believe that the mechanism of growth involves diffusion of ions through an electrolyte-saturated porous layer rather than ionic transport through a compact film. The porosity of the films formed in this study explains why the surface films do not inhibit current in this region. Thus, for example, currents on the cathodic sweep are larger than the corresponding currents on the anodic sweep. This contrasts with the situation at lower potentials where more compact films are formed, which impose some inhibition to the current flow.

### *Oscillatory behaviour*

As noted earlier, an interesting feature of the anodic potential sweep in Fig. 3 is the presence of current oscillations. Such oscillations appear on the forward sweep of the cyclic voltammograms when the upper limit, $E_U$, is greater than 1.7 V. They also appear on the reverse sweep when $1.7\,V < E_U < 2.4\,V$. As can be seen from Fig. 3, the current increases rapidly when the potential rises above 1.7 V, and so

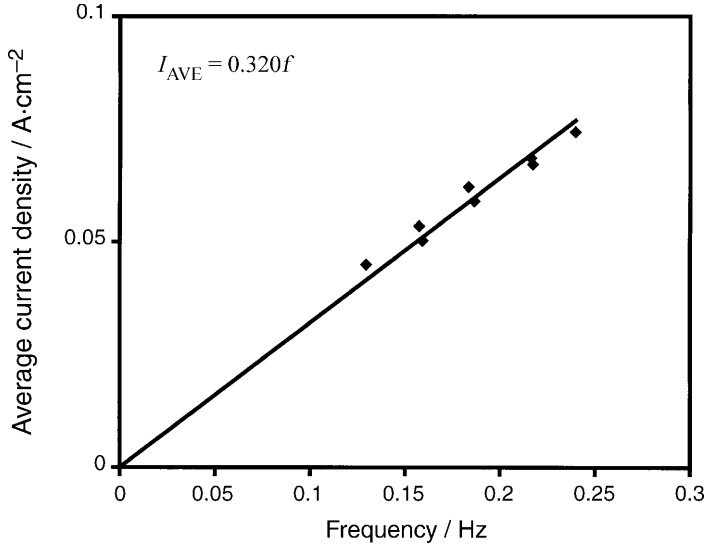


**Fig. 6.** Average current density plotted against frequency of oscillation under potential sweep conditions; the data were obtained from the cyclic voltammogram shown in Fig. 3

does the frequency of the oscillations. The relationship of the frequency of oscillation to the magnitude of the current was investigated by plotting the average current density against the observed oscillation frequency for a number of voltammograms. The data from one such voltammogram are plotted in Fig. 6 and yield a straight line through the origin.

This indicates that the charge per cycle is constant, with a value of $0.320\,C \cdot cm^{-2}$ given by the slope of the line. Thus, as the potential increases in a voltammogram from 1.7 to 2.4 V and the current increases correspondingly, the charge per cycle remains constant, and the frequency of oscillation increases.

Whereas the frequency range of the oscillations obtained from a given voltammogram is small, increasing the scan rate results, as expected, in an increase in the average current density with a corresponding increase in the frequency. A series of experiments was carried out in which the scan rate was varied from 0.001 to $0.1\,V \cdot s^{-1}$. The measured frequencies of the oscillations are listed in Table 1 and span the range from 0.1 to 1.25 Hz, the charge per cycle remaining constant

**Table 1.** Frequency range and charge per cycle measured from cyclic voltammograms carried out at various scan rates; the average value of charge per cycle is $0.323\,C \cdot cm^{-2}$ with a standard deviation of $0.010\,C \cdot cm^{-2}$

| Scanrate/$V \cdot s^{-1}$ | Observed frequency range/Hz | Charge per cycle/$C \cdot cm^{-2}$ |
|---|---|---|
| 0.001 | 0.10–0.17 | 0.34 |
| 0.005 | 0.16–0.29 | 0.32 |
| 0.01 | 0.15–0.32 | 0.32 |
| 0.02 | 0.29–0.59 | 0.32 |
| 0.05 | 0.54–0.93 | 0.33 |
| 0.1 | 0.73–1.25 | 0.31 |

within experimental error with an average value of $0.323\,C \cdot cm^{-2}$ and a standard deviation of $0.010\,C \cdot cm^{-2}$. Thus it is clear that, over a significant range of current density and frequency, the charge per cycle remains constant. The reasons for this are currently being investigated, and a more detailed analysis will be given in a future publication.

Oscillations of the current were also observed under constant potential conditions. Again a critical potential exists above which oscillations in the current density were observed. This potential is close to the value above which oscillations are observed in the cyclic voltammograms (*i.e.* approximately 1.7 V). A series of experiments was carried out in which the potential was stepped from open circuit to progressively higher potential values in the range from 1.8 to 2.5 V. Typical results are shown in Fig. 7 in which the potential was stepped to 1.8 and 2.1 V, respectively.

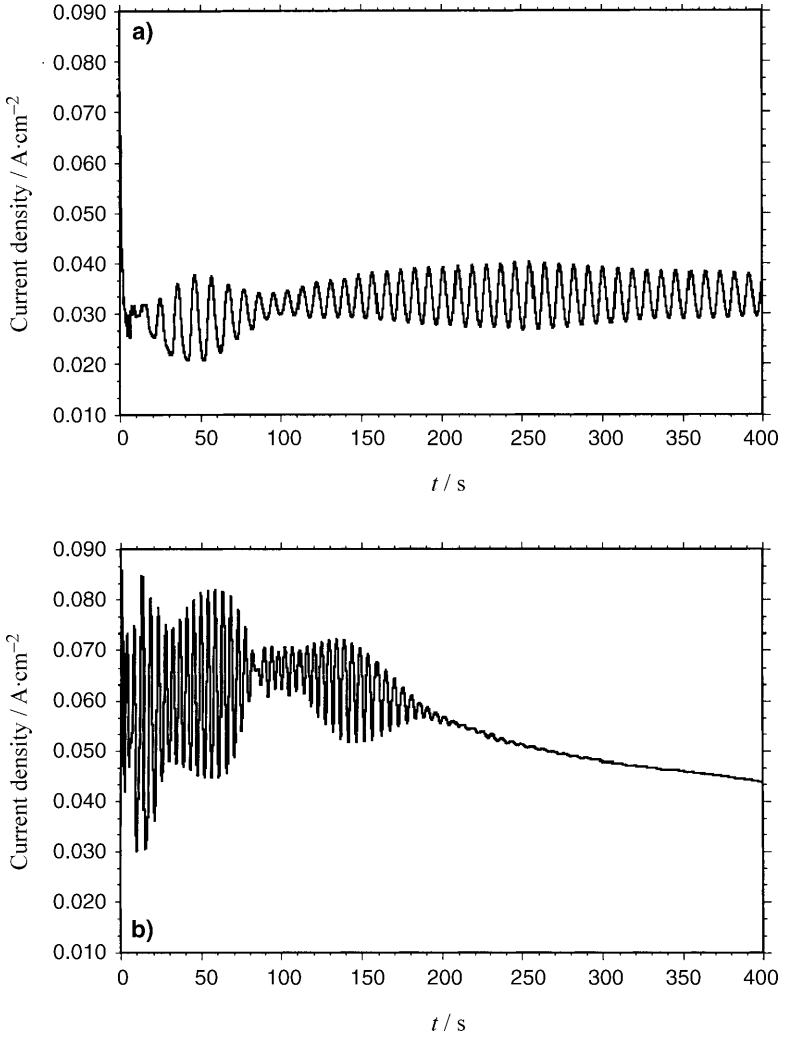


**Fig. 7.** Variation of current density with time at a constant potential of a) 1.8 and b) 2.1 V (SCE) in $3\,mol \cdot dm^{-3}$ $(NH_4)_2S$

Both curves show typical oscillatory behaviour. It is apparent from Fig. 7 that the average current density is higher after a potential step to 2.1 V and that the duration of the oscillations is longer for the lower imposed potential of 1.8 V. The charge per cycle also remained constant during these constant potential measurements: an average charge per cycle of $0.318\,C \cdot cm^{-2}$ was obtained. This is in good agreement with the value of $0.323\,C \cdot cm^{-2}$ given in Table 1 whose data originate from potentiodynamic measurements. Thus, for all values of the potential where oscillations were observed the average charge per cycle, estimated from the current *vs.* time curves, was found to be approximately constant, independent of the potential, and comparable in value to the constant charge per cycle estimated from the cyclic voltammetric measurements. Oscillations in potential under conditions of constant current were also observed and exhibited a complex signature.

*Mechanism of current oscillations*

The oscillatory behaviour in the Si/F system is often attributed to growth and dissolution of a thin surface film [37, 38] or changes in the surface roughness [39] of the film grown; *Carstensen et al.* [40] have developed a model which appears to agree well with experimental results. This model is based on an ionic breakthrough mechanism which leads to enhanced localized ion transport to the $Si–SiO_2$ interface. Under the conditions where oscillations occur in the present study, the InP electrode is covered by a thick (several microns) porous film that continues to thicken with increasing potential or time. This is much different from the Si/F system, in which the anodic films are of the order of tens of nanometres in thickness.

In metal/electrolyte systems, local changes in the *pH* and conditions for the formation and chemical dissolution of a passivating film are often associated with electrochemical oscillations [41, 42]. Some proposed mechanisms involve porous salt films and passivating oxides [43]. Cycling between two interface conditions as a consequence of diffusion or concentration gradients which cause cycling between high and low concentrations of $H^+$ and other species at the interface has been postulated. The case of copper in acidic chloride solutions is particularly interesting in the context of our results. In that case, *Bassett et al.* [44] have reported a thick porous film (in the order of tens of microns) on the electrode surface during the occurrence of oscillatory behaviour [44]. These authors also report a current-voltage behaviour similar to that observed by us for InP in the present study and postulate that oscillatory behaviour may be a consequence of the formation and dissolution of a thin oxide layer beneath the thick porous film.

In the present study, current densities are relatively high in the region where oscillations are observed. Consequently, relatively large changes in composition within the pores in the vicinity of the InP substrate are expected during current flow. For example, anodic dissolution of InP is accompanied by $H^+$ formation, and significant changes in *pH* are therefore expected. Similarly, the formation of $In^{3+}$ and oxo anions of phosphorus occurs, and water may even be depleted within the pores of the film adjacent to the InP. Under such conditions, the nucleation and growth of a solid phase resulting in a thin compact film at the interface of the InP and the porous film would not be surprising. This could lead to a rapid reduction

in current. After the current had decreased, the interphase region would recover due to the less polarizing influence of the lower current, and eventually the current would again increase. Such a scheme would provide the feedback mechanism essential for oscillatory behaviour.

Thus, although it is quite plausible that the oscillations are due to large changes in composition, including perhaps solid film formation at the interface of the InP and the porous surface film as outlined above, further work is required to explain the very regular and reproducible quantitative behaviour observed. An attractive feature of this proposed mechanism is that it may enable the extension of models developed for Si/F to the present system. We are currently working on a numerical model based on such a mechanism.

## *Conclusions*

The surface properties of InP electrodes were examined following anodization in an $(NH_4)_2S$ electrolyte. An observed current peak in the cyclic voltammogram was attributed to selective etching and film formation, and AFM images revealed surface pitting. Important for the understanding of passivation processes in sulfide solutions, two different types of surface film were observed to form depending on the applied potential. At lower potentials a compact film forms, whereas at higher potentials a transition from compact to porous film formation occurs.

Cracking of the surface film formed at potentials above 1.7 V was observed. The composition of this thick film was identified by EDX and XPS to be $In_2S_3$. It was demonstrated unambiguously by time-lapse optical microscopy that this cracking is not present when the electrode is removed from the cell but is an artifact of film drying. This is in contrast to the suggestion of *Gao et al.* [14] that similar cracking observed on p-type InP electrodes occurs *in situ* due to stress in the film during the anodization process. It is also clear that the cracking is a direct consequence of the porous, electrolyte-soaked nature of the film. Thus, an easy access pathway appears to exist for diffusion of ions between the substrate and the bulk electrolyte, and film growth is not inhibited. The film thickness was found to increase linearly with the charge passed, and quantitative estimates indicate that a constant percentage porosity of over 70% is maintained throughout the film.

Electrochemical oscillations were observed under three distinct and significantly different conditions: potential sweep, constant potential, and constant current. During potential sweep experiments at various scan rates, the average current density was found to be proportional to the frequency of the oscillations so as to sustain a constant charge per cycle of approximately $0.3\,C \cdot cm^{-2}$. Despite the differences in experimental conditions, current oscillations observed under constant potential conditions also showed a proportionality between average current and frequency and a similar value of approximately $0.3\,C \cdot cm^{-2}$ for the charge per cycle. The detailed mechanism of current oscillations is not clear. It is suggested that it involves large changes in electrolyte composition, including perhaps solid film formation at the interface of the InP and the porous surface film, similar in some respects to oscillatory processes on silicon in fluoride-based electrolytes.

## Experimental

The working electrode consisted of (100)-oriented monocrystalline sulfur-doped n-InP with a carrier concentration of approximately $4\times10^{18}\,\mathrm{cm}^{-3}$. An ohmic contact was established by alloying indium to the InP sample, and the contact was isolated from the electrolyte by means of a suitable varnish. Anodization was carried out in a $3\,\mathrm{mol}\cdot\mathrm{dm}^{-3}$ aqueous $(NH_4)_2S$ electrolyte, and a conventional three electrode configuration was used for the electrochemical experiments; all potentials are referenced to a saturated calomel reference electrode (SCE).

For cyclic voltammetric measurements and potentiostatic measurements, a CH Instruments Model 650 A electrochemical workstation interfaced to a PC was employed for cell parameter control and data acquisition. For constant current experiments, an EG&G Princeton Applied Research Model 363 potentiostat/galvanostat was used. All electrochemical experiments were carried out at room temperature and in the dark. The surfaces and cross-sections of the anodized samples were examined using a Nikon Nomarski optical microscope, a Joel JSM 840 scanning electron microscope, and a Topometrix atomic force microscope.

## Acknowledgements

*E. Harvey* gratefully acknowledges an Enterprise Ireland Research Scholarship.

## References

[1] Shaw DA and Thornton PR (1970) Solid State Electronics **13**: 919
[2] Sandroff CJ, Nottenberg RN, Bischoff JC, Bhat R (1987) Appl Phys Lett **51**: 33
[3] Gerard I, Simon N, Etcheberry A (2001) Appl Surf Sci **175–176**: 734
[4] Schmuki P, Spoule GI, Bardwell JA, Lu ZH, Graham MJ (1996) J Appl Phys **79**: 7303
[5] Eftekhari G (1994) Thin Solid Films **248**: 199
[6] Sumathi RR, Kumar MS, Dharmarasu N, Kumar J (1999) Matls Sci Engineer B **56**: 25
[7] Peng LH, Liao CH, Hsu YC, Jong CS, Huang CN, Ho JK, Chiu CC, Chen CY (2000) Appl Phys Lett **76**: 511
[8] Rotter T, Ferretti R, Mistele D, Fedler F, Klausing H, Stemmer J, Semchinova OK, Aderhold J, Graul J (2001) J Crystal Growth **230**: 602
[9] Elbahnasawy RF, McInerney JG (1999) In: Andricacos PC, Searson PC, Reidsema-Simpson C, Allongue P, Stickney JL, Oleszek GM (eds) Proceedings of Electrochemical Processing in ULSI Fabrication and Semiconductor/Metal Deposition II, PV 99-9. The Electrochemical Society, Proceedings Series, Pennington, NJ, p 242
[10] Yuzer H, Dogan H, Koroglu J, Kocakusak S (2000), Spectrochim Acta Part B **55B**: 991
[11] Bessolov VN, Konenkova EV, Lebedev MV, Zahn DRT (1999) Phys Solid State **41**: 793
[12] Wang Y, Dairici Y, Holloway PH (1992) J Appl Phys **71**: 2746
[13] Pang Z, Song KC, Mascher P, Simmons JG (1999) J Electrochem Soc **146**: 1946
[14] Huh C, Kim SW, Kim HS, Lee IH, Park SJ (2000) J Appl Phys **87**: 4591
[15] Yota J, Burrows VA (1993) J Vac Sci Technol A **11**: 1083
[16] Li ZS, Hou XY, Cai WZ, Wang W, Ding XM, Wang X (1995) J Appl Phys **78**: 2764
[17] Gao LJ, Bardwell JA, Lu ZH, Graham MJ, Norton PR (1995) J Electrochem Soc **142**: L14
[18] Marcu V, Tenne R (1988) J Phys Chem **92**: 7089
[19] Berlouis LEA, Elfick PV, Tarry H (1997) J Chem Soc Faraday Trans **93**: 2291
[20] Berlouis LEA, Peter LM, Greef R, Astles MG (1992) J Crystal Growth **117**: 918
[21] Van Meirhaeghe RL, Cardon F, Gomes WP (1979) Electrochim Acta **24**: 1047
[22] Blackwood DJ, Borazio A, Greef R, Peter LM, Stumper J (1992) Electrochim Acta **37**: 889
[23] Aggour M, Giersig M, Lewerenz HJ (1995) J Electroanal Chem **383**: 67

[24] Langa S, Carstensen J, Tiginyanu, Christophersen M, Foll H (2001) Electrochem Solid-State Lett **4**: G50
[25] Fenollosa R, You H, Chu Y, Parkhutik V (2000) Matls Sci Eng A **288**: 235
[26] Sazou D, Pagitsas M (1992) J Electroanal Chem **323**: 247
[27] Sazou D (1997) Electrochim Acta **42**: 627
[28] Wang C, Chen S, Yu X (1994) Electrochim Acta **39**: 577
[29] Harvey E, Buckley DN (2000) In: Kopf RF, Baca AG, Chu SNG (eds) Proceedings of the 32nd State-of-the-Art Program on Compound Semiconductors PV 2000-1. The Electrochemical Society, Proceedings Series, Pennington, NJ, p 265
[30] Harvey E, O'Dwyer C, Melly T, Buckley DN, Cunnane VJ, Sutton D, Newcomb SB, Chu SNG (2001) In: Chang PC, Chu SNG, Buckley DN (eds) Proceedings of the 35th State-of-the-Art Program on Compound Semiconductors PV 2001-2. The Electrochemical Society, Proceedings Series, Pennington, NJ, p 87
[31] Tao Y, Yelon A, Sacher E, Lu ZH, Graham MJ (1992) Appl Phys Lett **60**: 2669
[32] Lide DR (ed) (2000) CRC Handbook of Chemistry and Physics, 81st edn. CRC Press, NY
[33] Harvey E, Buckley DN, Sutton D, Newcomb SB, Chu SNG, J Electrochem Soc (submitted)
[34] Rappich J (2000) Microelectronics Reliability **40**: 815
[35] Spitzer SM, Schwartz B, Weigle GD (1975) J Electrochem Soc **122**: 397
[36] Robach Y, Joseph J, Bergignat E, Hollinger G (1989) J Electrochem Soc **136**: 2957
[37] Dini D, Cattarin S, Decker F (1998) J Electroanal Chem **446**: 7
[38] Cattarin S, Chazalviel JN, Da Fonseca C, Ozanam F, Peter LM, Schlichthorl G, Stumper J (1998) J Electrochem Soc **145**: 498
[39] Nast O, Rauscher S, Jungblit J, Lewerenz HJ (1998) J Electroanal Chem **422**: 169
[40] Carstensen J, Prange R, Foll H (1999) J Electrochem Soc **146**: 1134
[41] Russell P, Newman J (1986) J Electrochem Soc **133**: 2093
[42] Rush B, Newman J (1995) J Electrochem Soc **142**: 3770
[43] Beck TR (1982) J Electrochem Soc **129**: 2412
[44] Bassett MR, Hudson JL (1990) J Electrochem Soc **137**: 922

*Received October 16, 2001. Accepted (revised) December 21, 2001*